

# A LUT-based Method for Recovering Color Signals from High Dynamic Range Images

Keita Hirai and Shoji Tominaga

Graduate School of Advanced Integration Science, Chiba University, Chiba, Japan

## Abstract

*This paper describes an effective method for recovering color signals from multiband images of a high dynamic range (HDR) scene. We note that the color signals in a natural scene have the HDR characteristic of luminance level from very dark shadow area to highly bright sky. The Wiener estimator can be used for estimating spectral-power distributions of the color signals from HDR image data. A previous study presented an improved Wiener estimator for addressing accurate color signal estimation in HDR scenes. However, the previous method required the pixel-by-pixel estimation of parameters contained in the Wiener estimator, which resulted in requiring much computation time. For fast computation, therefore, we propose a lookup-table-based (LUT-based) estimation method for color signals in HDR scenes. In the preliminary stage in advance of color signal estimation, we prepare LUT of the statistical matrix needed in the Wiener estimator, consisting of the covariance matrix of color signals and imaging noises. In the stage of color signal estimation, the estimates are obtained pixel by pixel by the Wiener estimator with the most suitable matrix selected from the LUT. For validating the proposed method, experiments are conducted using actual HDR scenes. Experimental results show the superiority of our method in computation time to the previous methods, with keeping estimation accuracy.*

## Introduction

Spectral analysis of a variety of color signals in a natural scene is definitely one of the most important research problems in the recent color image science and technology [1-5]. This problem often includes (1) acquisition of high dynamic range (HDR) spectral images in outdoor natural scenes and (2) estimation of color signals from the image data [6]. Color signals of incident light into an imaging system consist of the direct spectra of light sources and the indirect spectra of the reflected lights from different object surfaces in a scene. The color signals in an HDR scene have the wide range of luminance level from very dark shadow area to highly bright sky. Therefore the problem of color signal reconstruction requires an HDR technique [7].

So far many estimation methods were proposed for estimating the color signals from image sensor outputs [8-11]. The Wiener estimator is well known and widely utilized for recovering spectral information from noisy observations. This estimator requires prior statistical parameters such as the covariance matrix of spectral dataset and the covariance matrix of imaging noise. These statistical parameters significantly affect the estimation accuracy. Therefore there were many attempts to determine suitably the statistical data in advance [12-18].

Most of the previous works addressed the spectral estimation, not in HDR scenes but in limited dynamic range scenes or low

dynamic range (LDR) scenes. Therefore it should be noted that the same estimator with fixed statistical parameters was applied to every pixel of the entire image in a natural scene. On the other hand, HDR scenes contain a huge difference in pixel values. So the statistical parameters should be determined dependently on the luminance level of the scene. For instance, the covariance matrix of color signals is determined using two databases of surface-spectral reflectances and light source spectra. Also the noise characteristics in HDR images are significantly different from the ones in LDR images. Then, the spectral databases and the imaging noise are suitably determined for HDR images. In 2011, Hirai et al. proposed a method for determining the statistical parameters of imaging noises and color signal dataset in order to estimate accurate color signals in an HDR scene [19]. They determined the suitable statistical parameters pixel by pixel, and applied them to the Wiener estimator. However, the previous method required much computation time because of the pixel-by-pixel parameter determinations.

The present paper describes a fast and accurate method for recovering color signals in HDR scenes. Our method is based on the lookup-table-based (LUT-based) Wiener estimation. In advance of color signal estimation, the suitable statistical parameters of imaging noises and color signal dataset are preliminarily calculated and stored in the form of LUT. In the estimation stage, a color signal in each pixel is recovered by using a suitable estimation matrix in the LUT. Finally, the feasibility of the proposed method is examined in real HDR scenes.

## Wiener Estimation for HDR scenes

An improved Wiener estimator was presented for HDR scenes [19], where the noise parameters were obtained by a imaging noise model of HDR images. The previous paper also determined luminance scale and color temperature for suitable color signal database. Color signals were then recovered pixel by pixel by the original Wiener estimator with the covariance matrix of the suitable color signal dataset and the covariance matrix of the estimated imaging noises. The pixel-by-pixel estimation method in the previous study is briefly described below.

### Original Wiener Estimator

The image sensor outputs are modeled as a following linear system.

$$\begin{aligned}\rho_i(\mathbf{x}) &= \int E(\lambda)R_i(\mathbf{x},\lambda)d\lambda + \sigma_i(\mathbf{x}) \\ &= s_i(\mathbf{x}) + \sigma_i(\mathbf{x}),\end{aligned}\tag{1}$$
$$i = 1, \dots, m,$$

where  $E(\lambda)$  denotes the incident color signal into an imaging system, and  $R_i(\lambda)$ ,  $s_i$  and  $\sigma_i$  are the spectral sensitivity function, the noise-free signal component, and the imaging noise of the  $i$ -th

sensor, respectively.  $\mathbf{x}$  is the spatial coordinates on an image. Then we can rewrite Eq.(1) in a matrix form:

$$\begin{aligned}\boldsymbol{\rho} &= \mathbf{R}\mathbf{e} + \boldsymbol{\sigma} \\ &= \mathbf{s} + \boldsymbol{\sigma},\end{aligned}\quad (2)$$

where  $\mathbf{e}$  denotes the  $n$ -dimensional vector representing the color signal  $E(\lambda)$  when sampling spectral functions at  $n$  points in the visible wavelength of [400, 700nm]. Also  $\mathbf{R}$  is a diagonal matrix with the size of  $m \times n$  for the spectral sensitivity function,  $\boldsymbol{\rho}$  is the  $m$ -dimensional sensor output,  $\boldsymbol{\sigma}$  is the  $m$ -dimensional noise vector, and  $\mathbf{s}$  is a  $m$ -dimensional signals.

When color signal  $\mathbf{e}$  and noise  $\boldsymbol{\sigma}$  are uncorrelated, the estimated color signal  $\hat{\mathbf{e}}$  is given by

$$\hat{\mathbf{e}} = \bar{\mathbf{e}} + \mathbf{W}(\boldsymbol{\rho} - \mathbf{R}\bar{\mathbf{e}}), \quad (3)$$

$$\mathbf{W} = \mathbf{C}_{ss}\mathbf{R}^t(\mathbf{R}\mathbf{C}_{ss}\mathbf{R}^t + \boldsymbol{\Sigma})^{-1},$$

where  $\bar{\mathbf{e}}$  is an average color signal of dataset,  $\mathbf{C}_{ss}$  is the covariance matrix of color signal dataset and  $\boldsymbol{\Sigma}$  is the covariance matrix of imaging noises as follows.

$$\begin{aligned}\mathbf{C}_{ss} &= E[(\mathbf{e} - \bar{\mathbf{e}})(\mathbf{e} - \bar{\mathbf{e}})^t], \\ \boldsymbol{\Sigma} &= E[\boldsymbol{\sigma}\boldsymbol{\sigma}^t].\end{aligned}\quad (4)$$

In the estimation, we can assume that the noises in each spectral channel are statistically independent. In this case, the covariance matrix of noises is reduced to be diagonal as

$$\boldsymbol{\Sigma} = \text{diag}(\sigma_1^2, \sigma_2^2, \dots, \sigma_m^2). \quad (5)$$

From Eq. (3), we can see the Wiener estimator is mainly characterized by three matrices:  $\mathbf{R}$ ,  $\mathbf{C}_{ss}$  and  $\boldsymbol{\Sigma}$ . In general,  $\mathbf{R}$  and  $\boldsymbol{\Sigma}$  are fixed for the imaging system.  $\mathbf{C}_{ss}$  is usually calculated from color signal dataset. In the previous study, as described in the later sections, the  $\mathbf{C}_{ss}$  and  $\boldsymbol{\Sigma}$  are suitably determined pixel by pixel.

### Noise Estimation of HDR Images

In the previous study, a noise model of HDR images is constructed by measuring the noise characteristics of raw image data captured by a linear system. First, the study showed the noises of raw LDR images have linear characteristic to signal components. We note that HDR images can be acquired by replacing the saturated pixels of long exposure images with the ones of short exposure images (See also later section “HDR Image Synthesis”). In this process, the pixel values of a short exposure image are multiplied by the ratio of the exposure time. This process means that, in the HDR image synthesis, the noise levels increase as well as the sensor outputs. Based on this observation, the previous work provided the linear noise model for HDR images as follows.

$$\sigma_i = a s_i + c_i b, \quad (6)$$

where  $a$  and  $b$  are the coefficients of the linear noise model, and  $c_i$  is the ratio of the exposure time which used in HDR image synthesis. Then by using Eqs.(1) and (6), the noises of HDR images can be rewritten as follows.

$$\begin{aligned}\sigma_i &= \rho_i - s_i, \\ s_i &= \frac{\rho_i - c_i b}{1 + a}.\end{aligned}\quad (7)$$

Then the estimated noises in an HDR image  $\hat{\sigma}_i$  can be calculated from the sensor outputs by the following equation.

$$\hat{\sigma}_i = \frac{a\rho_i + c_i b}{1 + a}. \quad (8)$$

Finally, the following noise covariance matrix for a pixel of an

input HDR image is calculated and applied to the Wiener estimator.

$$\boldsymbol{\Sigma} = \text{diag}(\hat{\sigma}_1^2, \hat{\sigma}_2^2, \dots, \hat{\sigma}_m^2). \quad (9)$$

### Suitable Color Signal Dataset for HDR Scenes

The accuracy of Wiener estimation depends on color signal dataset [14, 18]. In general, color signal database is generated by multiplying the surface-spectral reflectances and the illuminant spectra. However, in HDR scenes, the illuminant power scale and the color temperature significantly affect sensor outputs. Then the previous work acquired the suitable illuminant scale and color temperature in each pixel, and applied them for generating the suitable covariance matrix of color signal dataset,  $\mathbf{C}_{ss}$ , as follows.

$$\begin{aligned}\mathbf{C}_{ss} &= E[(\mathbf{e}_s - \bar{\mathbf{e}}_s)(\mathbf{e}_s - \bar{\mathbf{e}}_s)^t], \\ \mathbf{e}_s &= c_s \mathbf{E}_s \mathbf{r}, \\ \bar{\mathbf{e}}_s &= c_s \mathbf{E}_s \bar{\mathbf{r}},\end{aligned}\quad (10)$$

where  $c_s$  is the suitable illuminant power scale, and  $\mathbf{E}_s$  is the illuminant spectra of suitable color temperature.  $\mathbf{r}$  and  $\bar{\mathbf{r}}$  denote the reflectance database and its average.

### LUT-based Color Signal Estimation

The previous method determined the suitable parameters pixel by pixel, then the much computation time is required. On the other hand, we obtained the suitable parameters in the preliminary stage. Figure 1 shows the overview of our color signal estimation. In the preliminary stage in advance of color signal estimation, we prepare a possible dataset of  $xy$  chromaticity coordinates of color signals using the databases of surface-spectral reflectances and illuminant light sources. Then an input multiband HDR image is clustered based on the luminance level and the chromaticity coordinates. Then by using the representative luminance and chromaticity of each cluster, the statistical matrix needed in the Wiener estimator,

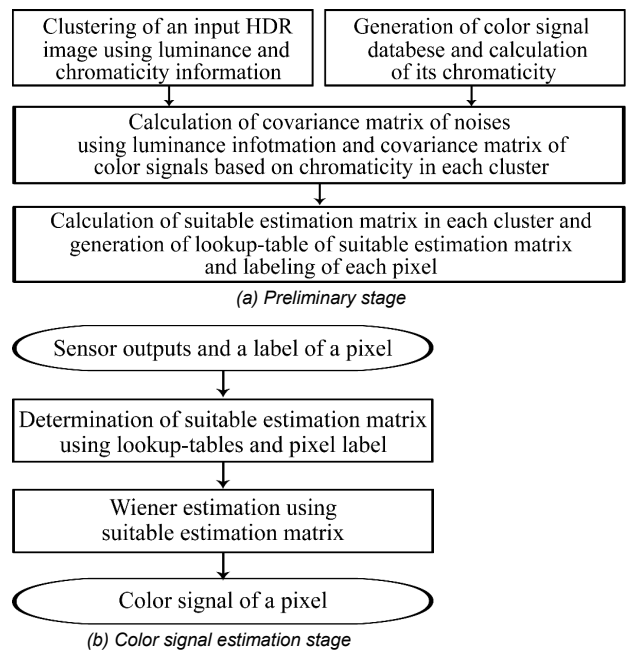


Figure 1. Overview of our LUT-based color signal estimation.

consisting of the covariance matrices of the color signals and the imaging noises, is determined in each cluster. The whole set of the statistical estimation matrices for the input HDR image is stored in the form of LUT. In the estimation stage, a color signal in each pixel is recovered by using a suitable estimation matrix in the LUT. In the following section, we describe the details of the proposed method from image acquisition to color signal recovery.

### Imaging System and HDR Image Synthesis

We use an imaging system for capturing multiband images, and a spectro-radiometer for directly acquiring illuminant spectral-power distribution in a particular region of a scene. The imaging system consists of a trichromatic digital camera and two color filters. The camera is a Canon EOS 1Ds Mark II with the linear response characteristic and the bit depth of 12 bits. The two additional color filters with different characteristics of spectral transmittance are used for multi-spectral image acquisition. By combining these color filters to the camera sensitivities, we can obtain six-band images. Figure 2 shows the overall spectral sensitivity functions of our imaging system. In our actual calculation, we sample all spectral functions at 61 equally wavelength points in visible range of [400, 700nm].

An HDR image is acquired conveniently by combing multiple LDR images captured at different exposure times [7]. Since our imaging system has linear response characteristics, the sensor outputs (pixel values)  $\rho$  at two different exposure times satisfy a relationship as

$$\rho^{(1)}(\mathbf{x}) = \frac{t(1)}{t(2)} \rho^{(2)}(\mathbf{x}), \quad (11)$$

where  $\rho^{(1)}$  and  $\rho^{(2)}$  are the sensor outputs at exposure times  $t(1)$  and  $t(2)$ . Based on this relationship, an HDR image can be obtained from LDR images as follows.

$$\rho_{HDR}(\mathbf{x}) = \begin{cases} \rho^{(1)}(\mathbf{x}) & (\rho^{(1)}(\mathbf{x}) \leq \tau) \\ \frac{t(1)}{t(j)} \rho^{(j)}(\mathbf{x}) & \left( \frac{t(1)}{t(j-1)} \tau < \frac{t(1)}{t(j)} \rho^{(j)}(\mathbf{x}) \leq \frac{t(1)}{t(j)} \tau \right) \\ \frac{t(1)}{t(m)} \rho^{(m)}(\mathbf{x}) & \left( \frac{t(1)}{t(h-1)} \tau < \frac{t(1)}{t(h)} \rho^{(h)}(\mathbf{x}) \right) \end{cases}, \quad (12)$$

$j = 2, \dots, h-1,$

where  $\tau$  is the threshold for clipping saturated pixels,  $h$  is the number of LDR images, and  $t$  is exposure time ( $t(1) > \dots > t(h)$ ). In later experiments, we set  $\tau = 3500$ .

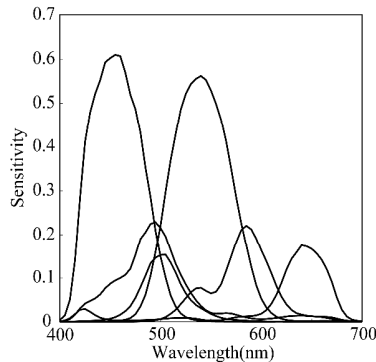


Figure 2. Spectral sensitivity functions of the six-band imaging system.

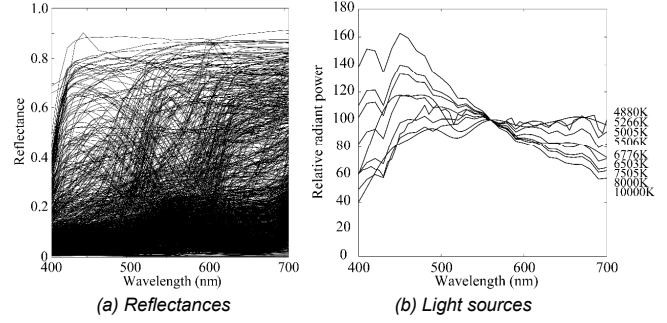


Figure 3. Spectral function databases.

### Color Signal Database

Figure 3(a) shows a set of our 1378 surface-spectral reflectance dataset for natural objects and artificial objects. Figure 3(b) shows an illuminant database consisting of nine light sources, which are the CIE standard spectral-power distributions of daylights with different correlated color temperatures from 5000K to 10000K [20] and the measured spectral-power distribution of daylight by using the spectro-radiometer.

Color signal dataset is generated by multiplying the surface-spectral reflectances and the illuminant spectra. Then, we obtain the color signal database with the size of 1378 x 9 color signals. Also we calculate  $xy$  chromaticities of the whole color signals for generating suitable color signal dataset (See later section "Generating Lookup-table of Estimation Matrix").

### Clustering using Luminance and Chromaticity

We employ luminance and chromaticity in CIE  $xyY$  color space for the clustering. As described in the previous section, noises of an HDR image are depended on the sensor outputs. In other words, scene luminance level is important to determine a suitable noise covariance matrix in the Wiener estimator, because scene luminance is significantly related with sensor output levels. Also, for determining suitable color signal dataset, it is required to select suitable samples from the whole set of color signal database. We can assume that if a color signal of an input pixel is similar to one in the database, the  $xy$  chromaticity of the input pixel is also similar to the one of in the database. Then, we select suitable color signal samples by using  $xy$  chromaticity.

First, we convert an input six-band HDR image to an image on the CIEXYZ color space as follow.

$$\begin{bmatrix} X \\ Y \\ Z \end{bmatrix} = \mathbf{M}\rho, \quad \mathbf{M} = \begin{bmatrix} \bar{x} \\ \bar{y} \\ \bar{z} \end{bmatrix} \mathbf{R}^T (\mathbf{R}\mathbf{R}^T)^{-1} \quad (13)$$

where  $\bar{x}$ ,  $\bar{y}$ , and  $\bar{z}$  are the  $1 \times 61$  vector representations of the color matching functions. Then,  $xyY$  values of the image are calculated.

In our study, we cluster the input image not in  $xyY$  three-dimensional space, but  $Y$  and  $xy$  space, separately. This is because the proposed method should ensure suitable noise covariance matrices which are determined based on suitable scene luminance levels. If we cluster the input image in  $xyY$  three-dimensional space, we have possibility that suitable scene luminance levels cannot be acquired by the clustering. In the clustering using luminance information, the input image is clustered based on equally-spaced  $Y$  values. In this process, the image is segmented into  $L$  clusters, and each luminance cluster is identified by a label  $l$  ( $l = 1, \dots, L$ ).

In the clustering based on chromaticity, we applied k-means clustering for the  $xy$  chromaticities of the input image. In this process, the image is segmented into  $K$  clusters, and each chromaticity cluster is identified by a label  $k$  ( $k = 1, \dots, K$ ). As a result, an input image is clustered into the  $L \times K$  clusters, and each cluster is identified by a label  $(l, k)$ .

### Generating Lookup-table of Estimation Matrix

**Determination of a noise covariance matrix in each cluster:** For calculating the suitable imaging noises in each cluster, we applied average sensor outputs in a cluster to Eq.(8) as follows.

$$\hat{\sigma}_i^{(l,k)} = \frac{a\bar{\rho}_i^{(l,k)} + c_i b}{1+a}, \quad (14)$$

where the index  $(l, k)$  denotes a cluster decided by a luminance cluster  $l$  and a chromaticity cluster  $k$ , respectively, and  $\bar{\rho}_i^{(l,k)}$  is a average sensor output in the cluster  $(l, k)$ . In our actual imaging system, the coefficients  $a$  and  $b$  are set as 0.011 and 4.35, respectively. Then, by using Eqs.(9) and (14), we acquire the suitable noise covariance matrix  $\Sigma^{(l,k)}$  in the cluster  $(l, k)$ .

**Determination of suitable color signal samples in each cluster:** As shown in the previous section, we obtained the color signal database with  $1378 \times 9$  color signals. We also calculated  $xy$  chromaticities of the whole color signals in the database. We assume that if a color signal of an input pixel is similar to one in the database, the  $xy$  chromaticity of the input pixel is also similar to the one in the database. Here we calculate the Euclid distances of  $xy$  chromaticities in a chromaticity cluster  $l$ .

$$E = \sqrt{(x^k - x^d)^2 + (y^k - y^d)^2}, \quad (15)$$

where  $x^k$  and  $y^k$  denote the representative  $xy$  chromaticity in the cluster  $k$ , and  $x^d$  and  $y^d$  denote a  $xy$  chromaticity calculated from the color signal database. A previous work indicated 50 samples are enough for generating the covariance matrix of spectral dataset [14]. Therefore, for determining a suitable color signal dataset  $\mathbf{e}^k$  in each cluster, based on Eq.(15), we calculate the distances  $E$  between a  $xy$  chromaticity of a cluster  $k$  to all  $xy$  chromaticities in the color signal database. Then we select 50 color signals from the color signal database with  $1378 \times 9$  color signals.

In HDR scenes, the color signal power scale is also important [19]. Then it is necessary to determine the suitable power scale. For the determination in each cluster  $(l, k)$ , the scale suited to the sensor outputs is determined by the following procedure.

$$\begin{aligned} & \operatorname{argmin}_{c_s^k} \left( \left( \bar{\mathbf{p}}_c^{(l,k)} - \bar{\mathbf{p}}_a^{(l,k)} \right) \left( \bar{\mathbf{p}}_c^{(l,k)} - \bar{\mathbf{p}}_a^{(l,k)} \right)^t \right), \\ & \bar{\mathbf{p}}_c^{(l,k)} = \bar{\mathbf{s}}_c^{(l,k)} + \mathbf{n}_c^{(l,k)} = (1+a)\bar{\mathbf{s}}_c^{(l,k)} + c_i b, \\ & \bar{\mathbf{s}}_c^{(l,k)} = c_s^{(l,k)} \mathbf{R} \mathbf{e}^k, \end{aligned} \quad (16)$$

where  $c_s^{(l,k)}$  is a factor for adjusting the color signal power scale in the cluster  $(l, k)$ ,  $\mathbf{e}^k$  is the average vector of suitable color signals in the cluster  $k$ , and  $\bar{\mathbf{p}}_a^{(l,k)}$  is the average actual sensor output vector in the cluster  $(l, k)$ .

The scale factor  $c_s^{(l,k)}$  and the suitable color signal dataset  $\mathbf{e}^k$  are determined by the above procedure and applied for generating the covariance matrix.

$$\begin{aligned} \mathbf{C}_{ss}^{(l,k)} &= \mathbb{E}[(\mathbf{e}_s^{(l,k)} - \bar{\mathbf{e}}_s^{(l,k)})(\mathbf{e}_s^{(l,k)} - \bar{\mathbf{e}}_s^{(l,k)})^t], \\ \mathbf{e}_s^{(l,k)} &= c_s^{(l,k)} \mathbf{e}^k, \\ \bar{\mathbf{e}}_s^{(l,k)} &= c_s^{(l,k)} \bar{\mathbf{e}}^k. \end{aligned} \quad (17)$$

**Lookup-table for color signal estimation:** Finally, the estimation matrix  $\mathbf{W}^{(l,k)}$  in each cluster is calculated as follows.

$$\mathbf{W}^{(l,k)} = \mathbf{C}_{ss}^{(l,k)} \mathbf{R}^t (\mathbf{R} \mathbf{C}_{ss}^{(l,k)} \mathbf{R}^t + \Sigma^{(l,k)})^{-1}. \quad (18)$$

Then the  $L \times K$  estimation matrices  $\mathbf{W}^{(l,k)}$  are stored in the form of LUT for an input HDR image. Also for the estimation stage, and  $L \times K$  average color signals  $\bar{\mathbf{e}}_s^{(l,k)}$  in whole clusters of an input image and their labels are stored in the LUT.

### Color Signal Estimation using Lookup-table

In the color signal estimation stage, input pixels are estimated by Eqs.(3) and (18).

$$\hat{\mathbf{e}} = \bar{\mathbf{e}}_s^{(l,k)} + \mathbf{W}^{(l,k)} (\boldsymbol{\rho} - \mathbf{R} \bar{\mathbf{e}}_s^{(l,k)}). \quad (19)$$

In this process, a label of each pixel is used for selecting a suitable estimation matrix in the LUT.

## Experiments

### Experimental Setups

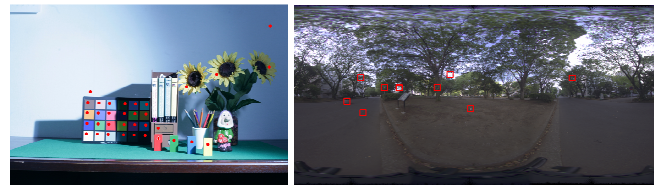
We used two HDR scenes shown in Fig.4, which include indoor and outdoor HDR scenes. HDR images are synthesized from the LDR images captured using the six spectral band imaging system described in the previous section. For measuring computation time properly, we resize the images to 100M pixels. The red points and squares in the images are the measurement spots by using the spectro-radiometer. The number of measurement spots in Fig.4(a) and (d) are 35 and 9 points, respectively. We also prepared a white reference in the scene and measured the spectra.

### Results

First, as shown in Table 1, we investigate relationships among the accuracy, the computation time and the number of clusters. The upper side of each cell denotes the normalized root mean square error (NRMSE), and the bottom side denotes the computation time. NRMSE is given by

$$NRMSE = \frac{\sqrt{\mathbb{E} \|\mathbf{e} - \hat{\mathbf{e}}\|^2}}{\sqrt{\mathbb{E} \|\mathbf{e}\|^2}}. \quad (20)$$

In general, CIELAB color difference is used for evaluating color accuracy. In this calculation, reference white is required. However, when using white reference in HDR scenes, CIELAB color difference often becomes very large values, and it is difficult to properly understand the color estimation accuracy. Therefore, we used NRMSE instead of CIELAB color difference. Our computer consists of 64bit-Linux OS, Core i7 990X, and 24GB memory. As shown in Table 1,  $L = 15$  and  $K = 10$  are enough for accurate estimation. On the other hand, the computation time are not significantly depended on the number of clusters. Therefore, in the next experiments, we set  $L = 20$  and  $K = 15$ .



(a) Scene #1 (b) Scene #2  
Figure 4. HDR scenes prepared in our experiments.

Next, for confirming the estimation accuracy of the proposed method, we implemented the two conventional estimation methods. One is the original Wiener estimator and the other is the previous improved Wiener estimator for HDR scenes [19]. In the original Wiener estimator, the noise is set at SNR = 40dB. Table 2 shows the comparative results between conventional and proposed methods. From these results, the estimation accuracy of the proposed method is approximately same as the previous method [19]. Also the computation time of the proposed method is approximately same as the original Wiener estimator, and much faster than the previous method [19]. Figure 5 and 6 show the measured and the estimated color signals of Fig.4(b). As shown in Fig.5 and 6, the proposed method can reproduce the accurate scales of color signals in HDR scenes.

**Table 1. Results of our proposed method when changing the number of clusters.**

	$L = 5$	$L = 10$	$L = 15$	$L = 20$
$K = 5$	0.323	0.292	0.289	0.287
	88.9 (sec)	89.5	90.5	90.9
$K = 10$	0.301	0.269	0.263	0.260
	89.3	89.8	91.2	91.4
$K = 15$	0.281	0.248	0.246	0.247
	89.7	90.2	91.1	91.6
$K = 20$	0.275	0.247	0.244	0.244
	90.1	90.8	91.5	92.1

**Table 2. Comparative results between conventional and proposed methods.**

	Original	Previous [19]	Proposed
NRMSE	0.415	0.236	0.244
Computation time (sec)	50.8	Approximately 7500	91.5

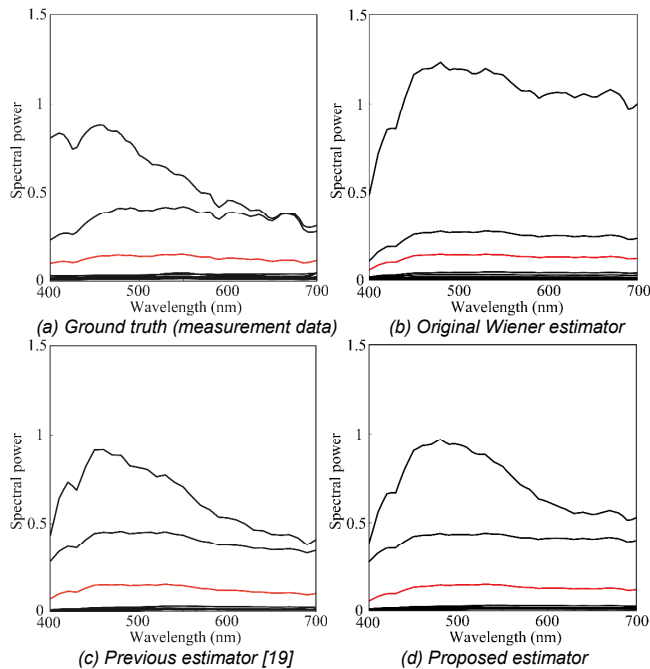


**Figure 5. Ground truth and estimated color signals of Fig.4(b). The figures are shown in wide horizontal axis scale. Red lines show the color signals of white reference which is utilized for normalizations.**

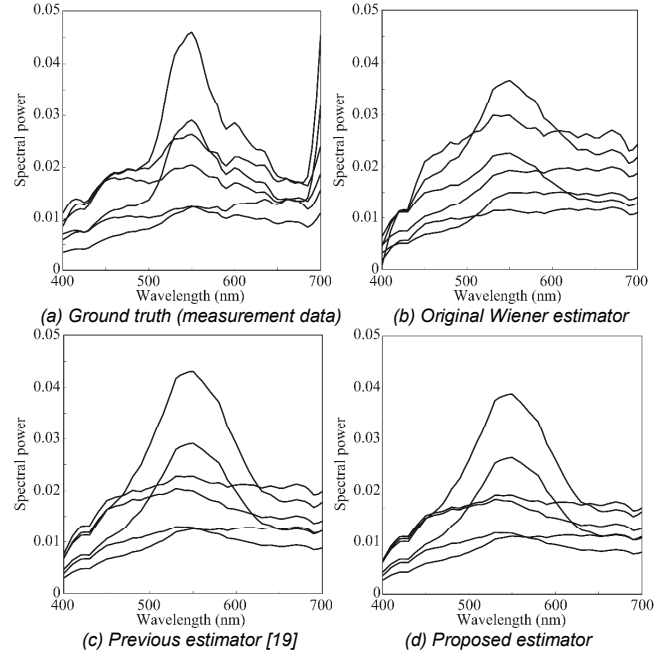


**Figure 6. Ground truth and estimated color signals of Fig.4(b). The figures are shown in narrow horizontal axis scale, compared to Fig.5.**

## Conclusions

This paper has described a LUT-based method for addressing fast and accurate color signal recovery in HDR scenes. In our method, the suitable statistical parameters in the Wiener estimator are calculated in advance of color signal estimation. In the preliminary stage, an input multiband HDR image is clustered based on luminance levels and chromaticity coordinates. Then, the statistical matrix consisting of the covariance matrices of color signals and imaging noises is determined by using the representative luminance and chromaticity of each cluster. The whole set of the statistical estimation matrices for an input HDR image is stored in the form of LUT. In the estimation stage, a color signal in each pixel is reconstructed by a suitable estimation matrix in the LUT. For validating our method, we conducted the experiments of the color signal estimations in actual HDR scenes. The experimental results showed the proposed method can provide fast and accurate color signal recovery, compared with the conventional estimation methods.

The proposed method has some parameters related with estimation accuracy: the number of luminance and chromaticity clusters, and the number of suitable color signals selected from the database. These parameters will be significantly influenced by scene dynamic range and contents. Therefore we would like to investigate the parameters of the proposed method in various scenes.

## References

- [1] C.C. Chiao, T.W. Cronin, and D. Osorio, "Color signals in natural scenes: characteristics of reflectance spectra and effects of natural illuminants," *J. Opt. Soc. Am. A*, **17**(2), 218-224 (2000).
- [2] C.C. Chiao, D. Osorio, M. Vorobyev, and T.W. Cronin, "Characterization of natural illuminants in forests and the use of digital video data to reconstruct illuminant spectra," *J. Opt. Soc. Am.*

- A, **17**(10), 1713-1721 (2000).
- [3] J. Hernández-Andrés, J.L. Nieves, E.M. Valero, and J. Romero, "Spectral-daylight recovery by use of only a few sensors," *J. Opt. Soc. Am. A*, **21**(1), 13-23 (2004).
- [4] E.M. Valero, J. L. Nieves, S.M.C. Nascimento, K. Amano, and D.H. Foster, "Recovering spectral data from natural scenes with an RGB digital camera and colored filters," *Color Res. Appl.*, **32**(5), 352-360 (2007).
- [5] O. Kohonen, J. Parkkinen, and T. Jääskeläinen, "Databases for spectral color science," *Color Res. Appl.*, **31**(5), 381-390 (2006).
- [6] S. Tominaga, A. Matsuura and T. Horiuchi, "Spectral analysis of omnidirectional illumination in a natural scene," *J. Imaging Sci. Technol.*, **54**(4), 040502-1 - 040502-9 (2010).
- [7] E. Reinhard, G. Ward, S. Pattanaik, and P. Debevec, *High dynamic range imaging: acquisition, display, and image-based lighting*, Morgan Kaufmann (2005).
- [8] S. Tominaga, "Multichannel vision system for estimating surface and illuminant functions," *J. Opt. Soc. Am. A*, **13**(11), 2163-2173 (1996).
- [9] P.D. Burns and R.S. Berns, "Analysis of multispectral image capture," *Proc. Fourth Color Imaging Conf. (CIC4)*, 19-22 (1996).
- [10] M. Hauta-Kasari, K. Miyazawa, S. Toyooka, and J. Parkkinen, "Spectral vision system for measuring color images," *J. Opt. Soc. Am. A*, **16**(10), 2352-2362 (1999).
- [11] H. Haneishi, T. Hasegawa, A. Hosoi, Y. Yokoyama, N. Tsumura, and Y. Miyake, "System design for accurately estimating the spectral reflectance of art paintings," *Appl. Opt.*, **39**(35), 6621-6632 (2000).
- [12] D. Dupont, "Study of the reconstruction of reflectance curves based on tristimulus values: comparison of methods of optimization," *Color Res. Appl.*, **27**(2), 88-99 (2002).
- [13] J.M. DiCarlo and B.A. Wandell, "Spectral estimation theory: beyond linear but before Bayesian," *J. Opt. Soc. Am. A*, **20**(7), 1261-1270 (2003).
- [14] H. Shen, P. Cai, S. Shao, and J.H. Xin, "Reflectance reconstruction for multispectral imaging by adaptive Wiener estimation," *Opt. Express*, **15**(23), 15545-15554 (2007).
- [15] Y. Murakami, M. Yamaguchi, and N. Ohya. "Piecewise Wiener estimation for reconstruction of spectral reflectance image by multipoint spectral measurement," *Appl. Opt.* **48**(11), 2188-2202 (2009).
- [16] Y. Murakami, M. Yamaguchi, and N. Ohya, "Class-based spectral reconstruction based on unmixing of low-resolution spectral information," *J. Opt. Soc. Am. A*, **28**(7), 1470-1481 (2011).
- [17] N. Shimano, "Noise analysis of a multispectral image acquisition system," *Proc. Fifth European Conf. on Color in Graphics, Imaging and Vision (CGIV)*, 523-528 (2010).
- [18] N. Shimano, and M. Hironaga, "Recovery of spectral reflectances of imaged objects by the use of features of spectral reflectances," *J. Opt. Soc. Am. A*, **27**(2), 251-258 (2010).
- [19] K. Hirai, and S. Tominaga, "Color signal estimation in high dynamic range scenes," *Proc. Nineteenth and Color Imaging Conf. (CIC19)*, 298-303 (2011).
- [20] G. Wyszecki, and W. S. Stiles, *Color Science: Concepts and Methods, Quantitative Data and Formulae*, 2nd Ed., Chap. 1, Wiley-Interscience, (2000).

## Author Biography

*Keita Hirai received the B.E., M.S. and Ph.D. degrees from Chiba University in 2005, 2007 and 2010. He was also a research fellow of Japan Society for the Promotion of Science (JSPS) from April 2009 to March 2010. He is currently an Assistant Professor of Graduate School of Advanced Integration Science, Chiba University, Japan. He is interested in the researches for visual information processing, color image processing, computer vision and computer graphics.*